PCCP

Accepted Manuscript




ROYAL SOCIETY OF CHEMISTRY

www.rsc.org/pccp

*Phys. Chem. Chem. Phys.*

RSCPublishing

ARTICLE

# Evidence of "new hot spots" from determining the nonlinear optical behavior of materials: mechanism studies on vanadium borate crystal $Na_3VO_2B_6O_{11}$

Cite this: DOI: 10.1039/x0xx00000x

Received ooth January 2014,
Accepted ooth January 2014

DOI: 10.1039/x0xx00000x

www.rsc.org/

Xin Su, [a b] Zhihua Yang,* [a] Ming-Hsein Lee,[c a] Shilie Pan,* [a] Ying Wang, [a b] Xiaoyun Fan, [a] Zhenjun Huang, [a b] Bingbing Zhang, [a b]

A novel mechanism for nonlinear optical (NLO) effect of vanadium borates crystal, $Na_3VO_2B_6O_{11}$ (NVB), with distorted $VO_4$ groups have been investigated. A comprehensive analysis for the structure-property relationship is given by combining the experimental measurements, the electronic structures calculations, the SHG-weighted electron density and the real-space atom-contribution analysis to the linear and nonlinear optical properties. It is found that the contribution of $(VO_4)^{3-}$ anionic group to the second harmonic generation (SHG) response is more pronounced than that of the $(BO_3)^{3-}$ anionic group, which play a virtual role to the SHG effects in NVB. And the anionic $(BO_3)^{3-}$ groups have dominant contributions to the birefringence, while the contribution of the $V^{5+}$ cations to this linear optical effects is negligibly small.

## Introduction

Borate materials which possess crystallographic noncentrosymmetric (NCS) are of great interest for their potential characters especially in second-order nonlinear optical (NLO) activity.[1-2, 3-17] Introducing NCS building units becomes one of extremely important ways to obtain NCS structures[18, 19-24], such as acentrically distorted units with octahedral coordinated $d^0$ transition metals ($Nb^{5+}$, $V^{5+}$, etc.) or lone-pair active cations ($Pb^{2+}$, $Bi^{3+}$) due to second-order Jahn-Teller (SOJT) effect.[25] While it is reported that SOJT distortions are not the only displacement presence in $d^0$ materials,[26] a $d^0$ transition metal cation may also distort tetragonally along *C*4 axis.[27] Introducing $d^0$ transition metal $V^{5+}$ into borates may promote the formation of new NCS borate materials. Several vanadium borates such as $Na_3VO_2B_6O_{11}$[28] and $K_2SrVB_5O_{12}$[29] with non-SOJT-type distortion have exhibited interesting NLO properties.

The existence of vanadium borate, $Na_3VO_4B_6O_9$ was first obtained in early 2000 by Touboul et al. in the course of their investigation of heating a mixture of $Na_2CO_3.H_2O$, $V_2O_5$, and $H_3BO_3$.[28] In 2010, the single crystal of $Na_3VO_4B_6O_9$ was grown and the crystal structure was described by our group.[30, 31, 32] The formula of $Na_3VO_4B_6O_9$ has been changed to $Na_3VO_2B_6O_{11}$ (NVB) according to its anionic structure.[32] NVB crystallizes in the space group of $P2_12_12_1$ with cell dimensions $a$ = 7.7359(4) Å, b = 18.744(9) Å, $c$ = 12.5697(0) Å, and $Z$ = 4. As shown in Figure 1, this structure has a three-dimensional framework which is built up of $B_6O_{11}$ units, $VO_4$ tetrahedra, $NaO_7$ and $NaO_8$ polyhedra. The hexa-borate $B_6O_{11}$ unit consists of three $BO_4$ units and three $BO_3$ units are joined together through corner-sharing O atom forming. The $VO_4$ tetrahedra and the sodium atoms are distributed in the channels of the two-dimensional (2D) network of B-O groups.[31]

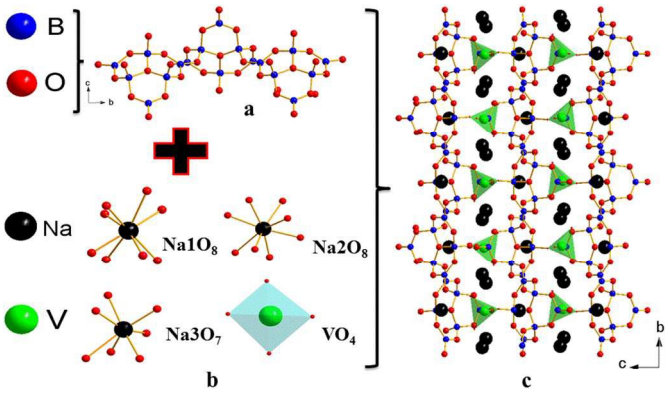


Figure 1. Ball-and-stick representation of NVB, $B_6O_{11}$, $VO_4$, $NaO_7$ and $NaO_8$ groups in the three-dimensional network. (a) $BO_3$ triangle and $BO_4$ form $B_6O_{11}$ polyhedra. (b) The different coordinations of the $NaO_n$ (n=7, 8) and $VO_4$ groups, respectively. (c) Black arrows represent the direction of two-dimensional network of NVB viewed down the *a*-axis. Na, V, B, O atoms are drawn as black, green, red and blue balls, respectively.

Recent investigations in our group on the linear and nonlinear optical (NLO) properties of NVB indicate that this crystal is a promising material for SHG effect and gives a similar response to that of KDP, a wide transparency range from 370 to 3000 nm with the shortest SHG wavelength at 427 nm. [32] Considering the origin of the NLO effects in NVB, it is interesting and meaningful to grow a large single crystal and further investigate its structure–property relationship. Since NVB was first reported by Touboul et al.,[28] to our best knowledge, no theoretical studies on the linear and NLO properties of NVB compound have been reported until now, and the mechanism of the SHG response for NVB is still an open problem. So far, a tentative viewpoint on the origin of the NLO effect of NVB is that there exist structure distortion and $d^0$ transition metal $V^{5+}$ in the $VO_4$ asymmetric coordination environments in the crystal.[31,32]

In recent years, *ab initio* energy-band calculations of linear and nonlinear optical effects for $\beta$-$BaB_2O_4$ (BBO),[33] $LiB_3O_5$ (LBO), $CsB_3O_5$ (CBO) and $CsLiB_6O_{10}$ (CLBO), [34] $KBe_2BO_3F$ (KBBF),[35] $BaAl_2B_2O_7$ (BABO), $K_2Al_2B_2O_7$ (KABO)[36] and $BiB_3O_6$ (BIBO),[37] $NaNO_2$,[38] and $KH_2PO_4$ (KDP)[39] et. al., with a satisfactory explanation for the mechanism of NLO effects. In this work, we employed CASTEP,[40] a plane-wave pseudopotential total energy package, to calculate the electronic band structures, linear and nonlinear optical properties of the NVB crystal. In addition, combined with the SHG-weighted electron density analysis and the real-space atom-cutting technique, we analyzed the respective contributions of various transitions among cations and anionic groups to the optical responses of NVB. In this contribution, we use the above calculation method to analyze the electronic band structures and the mechanism for the linear and nonlinear optical properties of the NVB family and obtain some useful results which are essential to the design and search for new NLO crystals. It is found that the virtual transition processes between the V cations and the neighbor O anions have much larger contributions to the SHG effects compared to the $(BO_3)^{3-}$ anionic groups, although the latter microscopic units have the dominant contribution to the birefringence in NVB.

### Methods and Computational Details

The first-principles calculations are performed by the plane wave pseudopotential method in the CASTEP package[40] based on the density functional theory (DFT).[41] In the present study, the generalized gradient approximation (GGA) with the Perdew–Burke–Ernzerhof (PBE) functional and the norm-conserving pseudopotential were adopted. [42-44] The kinetic energy cutoffs of 750.0 eV and Monkhorst-Pack *k*-point meshes[45] (4 × 3 × 3) with a density of 0.025 $Å^{-1}$ in the Brillouin zone (BZ) were chosen. Our convergence tests reveal that the above computational parameters are sufficiently accurate for present purposes. Moreover, to account for the effect of localized *d* orbitals in transition element, the LDA+U method with the on-site orbital dependent Hubbard U[46, 47] energy term for V is employed for the electronic structure calculations. Different U potentials from 2 to 10 eV for V atoms have been adopted for test calculations, and it turns out that its choice has little influence on the calculated optical properties since it just affects the position of V 3*d* orbitals mainly located in the energy region away from band gap. Although NVB crystals contain a transition metal V, there is no need in using U because the band gap is already reproduced fairly well. This result is similar to a recent study on another material YAB.[48]

The linear optical properties of NVB are determined by the frequency-dependent dielectric function $\varepsilon(\omega) = \varepsilon_1(\omega) + i\varepsilon_2(\omega)$ , which is mainly connected to the electronic structures. The imaginary part $\varepsilon_2(\omega)$ of the dielectric function $\varepsilon(\omega)$ is calculated from the momentum matrix elements between the occupied and unoccupied electronic states and given by: [49]

$$\varepsilon_2\left(\mathrm{q} \to O_{\dot{u}}, h\omega\right) = \frac{2e^2\pi}{\Omega\varepsilon_o}\sum_{kcv}\left|\left\langle\varphi_k^c\left|u\cdot r\right|\varphi_k^v\right\rangle\right|^2\delta\left[E_k^c - E_k^v - E\right]$$

The real part $\varepsilon_1(\omega)$ can be obtained from the imaginary part $\varepsilon_2(\omega)$ by the Kramers–Kronig transformation. All the other optical constants, such as the absorption spectrum, refractive index, and reflectivity are derived from $\varepsilon_1(\omega)$ and $\varepsilon_2(\omega)$.[50]

Furthermore, to analyse the contribution of the relevant groups to the linear and nonlinear optical properties, and to gain further insight into the structure-property relationship, the SHG-weighted electron densities analysis[51, 52] and real-space atom-cutting method[53] are adopted to analyse the origin of the nonlinear optical response of NVB for the first time. The theoretical methods have been applied with success to analyse the linear refractive indices and SHG coefficients of NLO crystals, in our previous study.[54-59]

## Results and Discussion

### A. $VO_4$ distortion

The geometric parameters of NVB crystal are given above[32] and the basic structural features are shown in Fig.1. To further improve the understanding of the structure-property relationships, we have analysed the structure of the distorted $VO_4$ tetrahedra. The distortions of $VO_4$ tetrahedra are influenced not only by the electronic structure of cation $V^{5+}$ but also by the structure of the bond network, lattice in-commensuration, and cation-cation repulsion, [53, 60] the probable reasons as follow: (1) In the lattices, the metal $V^{5+}$ ions occupying Wyckoff 4*a* positions employ the 4-fold $T_d$ site in the distorted tetrahedra environment of $(VO_4)^{3-}$, with a V−O bond length in the range of 1.6376 − 1.8557 Å. As a comparison, a similar result concerns the $VO_4$ tetrahedron, where the mean value 1.7265 Å (Table S1) corresponds to the mean values found in vanadate such as $CrVO_4$,[61] 1.7256 Å; $InVO_4$,[62] 1.7263 Å, $In_{0.6}Li_{1.2}VO_4$,[63, 64] 1.7220 Å and $CuMnVO_4$,[65] 1.7290Å. (2) The V−O(12), V−O(13) distances of 1.6600 and 1.6610 Å are all shorter than those of V−O(1) and V−O(2) of 1.8460, 1.7690 Å Figure S1. (3) The O(1)−V−O(2) angle of 120° is significantly deviated from 109° for a perfect tetrahedron, which is due to the polar displacement of a $d^0$ cations $V^{5+}$. The $VO_4$ with an apparent displacement from the center of the tetrahedron may become one dominant NLO active factor to the SHG response, which can be further quantitatively proved by the results via *ab initio* calculations of the SHG-density and the real-space atom-cutting method.

### B. Mulliken atomic populations analysis

To gain more insight on the bonding character and to explain the charge transfer in NVB we have calculated the Mulliken population analysis. The calculated result reveals that



 

the B-O and V–O bonds show more covalent character than other bonds (Table 1). A greater Mulliken atomic charge assures ionic bonding and smaller Mulliken atomic charge demonstrates the presence of a covalent bond between atoms. The atomic charge values of Na, B, O and V are 1.15 ~ 1.17, 0.79 ~ 0.83, -0.56 ~ -0.73 and 0.72, respectively. The charge transfers between O and Na are 1.94, larger than those between O and B, V, which indicates the ionic character of the bonds between O and Na atoms, covalent nature between O and B, V bonds. From the atomic charge we can find out the percentage ionic character.

Table 1. Mulliken charge population of $Na_3VO_2B_6O_{11}$.

| Atom | Na | B | O | V |
|---|---|---|---|---|
| population | 1.15 ~ 1.17 | 0.79 ~ 0.83 | -0.56 ~ -0.73 | 0.72 |

The bond distances and calculated Mulliken overlap populations Q are shown in Table 2, to better understand the bonding behavior of NVB. The bond order analysis shows that the Na-O, B-O and V-O bond have values of 0.03 ~ 0.07*e*, 0.56 ~ 0.88*e* and 0.50 ~ 0.82*e*, respectively. In NVB crystal, sodium is characterized by a small overlap population, which further indicates an ionic bond. Therefore, the B–O and V–O bonds show more covalent character than the Na–O bonds.

Table 2. Bond distances *d* and Mulliken overlap populations Q (|*e* |) for characteristic atomic pairs in $Na_3VO_2B_6O_{11}$.

| Value Atomic pair | bond distances *d* (Å) | overlap populations |
|---|---|---|
| Na-O | 2.6814(6) ~ 2.3930(3) | -0.03 ~ 0.07 |
| B-O | 1.5277(0) ~ 1.3683(7) | 0.56 ~ 0.88 |
| V-O | 1.8444(5) ~ 1.6604(2) | 0.50 ~ 0.82 |

**C. Band structure and density of states**

To perform electronic structure calculations, the experimental crystal structure were adopted initially and then computationally optimized, the resulting unit cell parameters and atomic positions were found to be close to those obtained from the experiment. The calculated electronic energy band structure along the high symmetry directions in the BZ, is displayed in Figure 2a. From Figure 2a, one can see that both the conduction band minimum (CBM) and the valence band maximum (VBM) are located at point Γ, resulting in a direct band gap of 3.28 eV (see Tables S2), while the corresponding experimental data is 3.35 eV. Moreover, we have tried to use other kinds of pseudopotentials to calculate the bands and found that the change of the results is not apparent.

As the value of the energy gap is an important issue for optical property, we therefore paid more attention to get the energy gap closer to the experimental values. To gain a deeper understanding of the band structure features, we plotted slices of orbital density of conduction bands (CB) and valence bands (VB) near the band gap as shown in Figure 2b. It is clear that the bands near the band gap are determined by V-O hybridization states sited at CB and the states from O and B sited at VB. Another result can also be observed is that V, B and the neighboring O atoms are characterized by strong overlap population, which indicates apparent covalence behaviors agreeing to Table 2.

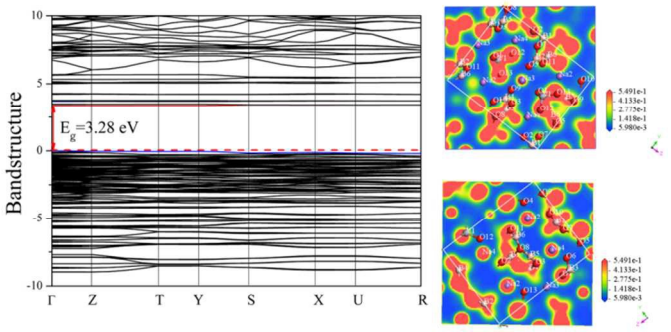


Figure 2. (a) Electronic band structure along high-symmetry k-points (Γ-Z-T-Y-S-X-U-R) of NVB (left), the highest occupied state is set to 0 eV. (b) And the corresponding projected wave function at special energy regions (right): the above and below diagrams are charge density contour projected of the VO group and BO group, respectively.

In the present theoretical calculation, transitions from occupied states to unoccupied states are considered. Useful information can be gained from partial density of states (PDOS), such as hybridization of states, bonding nature and contribution of orbitals to the electronic band structure. Figure 3a displays the density of states (DOS) and partial (PDOS) of the respective species in NVB. The electronic property is obtained by analysing the highest occupied orbitals and lowest unoccupied orbitals in conjunction with optimized atomic structures. The corresponding calculated optical absorption coefficient spectrum $\alpha$ is shown Figure 3b. We clearly see that the highest occupied and lowest unoccupied state levels respectively come from non-bonding O-2*p* from Fermi Level (FL) to about -0.8 eV and V-O orbits as shown in Figures 3c and 3*d*. The energy range from -0.8 to -3.0 eV in VB region has significant contributions from O-2*p* mixing with V-3*d* and B-2*p* states. In the energy region from -3.0 eV to -9.0 eV, however, the contributions of B-2*s* and B-2*p* are apparent in addition to O-2*p* states. As for CBs, the bands above the FL are mainly derived from V-3*d*, O-2*p*, B-2*p* states with slight contribution of *s* and *p* orbitals of Na. From figure 3, it is shown that electronic transitions from VBs to CBs mainly dominate the intrinsic UV absorption $\alpha$, which exhibits a lot of prominent peaks mainly owing to energy subbands. From figure 3 also concludes that the position of the non-bonding oxygen and V-O orbits has determined the band gap of NVB crystals.

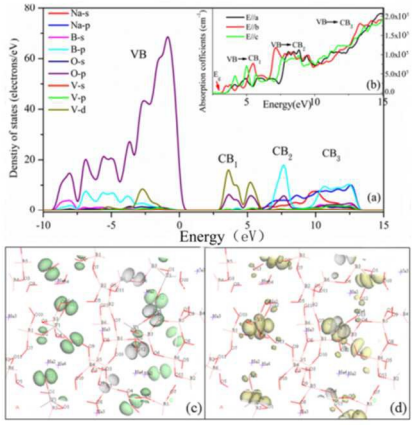


Figure 3. DOS (a), absorption spectrum (b), the energy range of the specific orbitals of the NVB crystals shown in (c) (d).

**D. Optical response**

The refractive indices measured by the minimum deviation technique show that NVB is a positive biaxial optical crystal. The calculated refractive indices consist with experimental ones, an obvious optical anisotropy characterized via $n^z$ - $n^x$ has been exhibited in Figure 4 and Table S3. The calculated and experimental dispersion curves of refractive indices also display a moderate birefringence around 0.05 at 1064 *nm*. For practical application of NLO crystals as a frequency converter, it should allow the fundamental radiation to stay in phase with those second-harmonic generated, i.e., the phase velocity must be the same for both the second harmonic and the fundamental waves.[66] The phase-matching conditions have been deduced from the calculated refractive indices, as shown in Supplementary Table 4, which confirms that NVB is phase matchable for SHG of 1064 and 532 nm lasers.

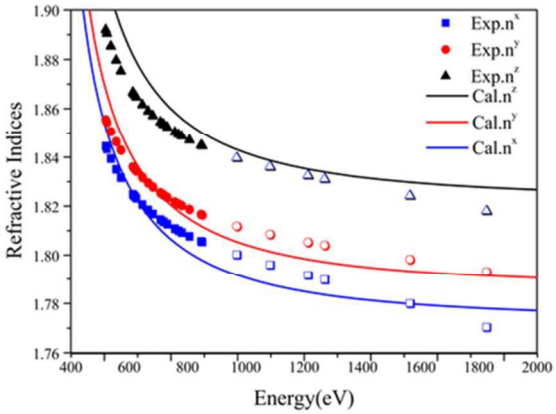


Figure 4. The calculated and experimental refractive index dispersion (White patterns several data were fitted using Sellmeier equations (see in Supporting Information Eqs. (2) - (4)).

The sum-over-states type formalism has been proposed to evaluate the SHG coefficients. [67, 68] We calculated the second-order coefficients $d_{ij}$ under the static limit within the length gauge.[69, 70] There are three nonzero components of the second-order polarizability tensor, namely $d_{14} = d_{25} = d_{36}$ due to the symmetry of NVB. The calculated SHG coefficient $|d_{14}|$ is 0.45 pm/V. The $|d_{\text{eff}}^{\text{SHG}}|$[71] of NVB crystal for type-I PM in ZX and YZ planes at 1064 *nm* fundamental wavelength are about 0.44 pm/V and 0.16 pm/V, respectively (formulas as shown in Table S4). These coefficients are very close to the experimental powder SHG effect value, about that of KDP ($KH_2PO_4$, $|d_{\text{eff}}^{\text{SHG}}| \approx 0.38$ pm/V). Herein, this agreement, as well as other accuracy test results shown in Figure S3 is reconfirmed the validity of our choice of gradient generalized approximation (GGA) approximation in current study.

**E. The SHG-weighted electron densities and real-space atom cutting**

We plot the SHG-weighted electron densities of NVB in Figure 5. Here we only consider the virtual-electron (VE) since they have dominant contributions to the SHG effects (almost 90% of the total value) in NVB.[72-74] In analogy to the alkali metal or alkali earth metal ions in the KBBF-type UV borate NLO crystals, including KBBF,[35] KABO, BABO,[36] and BABF,[52] the Na cations of NVB both in occupied and unoccupied states have strong ionic characteristics resulting in a spherical symmetric distribution, which shows almost no effect on SHG. The occupied states contributing to SHG mainly come from the B-2*p* and O-2*p* orbitals, while the unoccupied states mainly from the V-3*d* as well as partial B 2*p* orbitals. This means that the VE processes from the O valence states to the V and B conduction states determine the SHG effects in NVB.

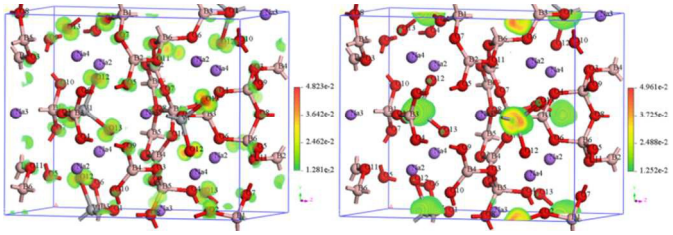

Figure 5. The occupied states (left) and unoccupied states (right) in $d_{14}$ SHG-densities of NVB crystal in the VE process.

In order to investigate the respective contributions of the anionic groups to the birefringence and SHG response of NVB, we employ the real-space atom-cutting method.[76] Based on the electron density and SHG-weighted electron density analysis results,[50, 77] the microscopic units can naturally be categorized as follows: the $Na^+$ cations, the $(BO_3)^{3-}$, $(BO_4)^{5-}$ groups, and the $(VO_4)^{3-}$ groups. The cutting radius of Na is 0.95Å by investigating the charge-density distribution between the nearest Na and O ions. Following the rule, the cutting radii for the boron, vanadium and oxygen atoms are chosen as 0.88Å, 1.2Å and 1.1Å, respectively. It is shown in Table 3 that the contribution of the $(VO_4)^{3-}$ group to the refractive indices is comparable to that of the $Na^+$ cations, the $(BO_3)^{3-}$, $(BO_4)^{5-}$ groups. Whereas the contributions of $(VO_4)^{3-}$ to the birefringence are only about 6.43%, the contributions of the $(BO_3)^{3-}$ and $(BO_4)^{5-}$ anionic groups are also about 46.70%, respectively. And the $Na^+$ cations contribute more than 11.55% to the anisotropy of refractive indices. The sum of the contributions from groups is larger than the original calculated value due to the repeated calculation of the wave-functions of some shared oxygen atoms, otherwise they should be nearly equal like situations in $KBe_2BO_3F_2$,with individual $BeO_3F$ and $BO_3$ groups.[68] The overlap calculation will not influence the contribution, therefore for the birefringence of NVB, the relations of the contribution are $(BO_4)^{5-} \sim (BO_3)^{3-} > Na^+ \sim (VO_4)^{3-}$.

Comparatively and interestingly, the contributions from ions and atomic groups to SHG response are very different from that to the refractive indices and birefringence. This atom-cutting analysis reveals quantitatively that the main SHG contribution from $(BO_3)^{3-}$ and $(VO_4)^{3-}$ groups is much larger than those from $Na^+$ cations and $(BO_4)^{5-}$ groups, and the corresponding contributions from the group $(VO_4)^{3-}$ and $(BO_3)^{3-}$ about 50.61% and 44.34% to the overall SHG coefficient, which are significant larger than other groups in NVB, with the sequence is $(VO_4)^{3-} > (BO_3)^{3-} > (BO_4)^{5-} > Na^+$ for SHG response. Therefore, as indicated in the above-mentioned discussions for NVB crystal, the $(BO_3)^{3-}$ or $(BO_4)^{5-}$ group is one but not the only one reason inducing the large NLO effects, which NLO effects mainly originate from "new hot spots" in NVB, $(VO_4)^{3-}$ anionic groups.

Table 3. The atom-cutting analysis result for the NVB crystal. The sum of the contributions from individual groups in the crystal is larger than the original calculated value of the whole crystal due to the repeated calculation of the wave-functions of some shared oxygen atoms.

| All $M^+$ in unit cell | $n^x$ | $n^y$ | $n^z$ | $\Delta n$ | $d_{14}$ (pm/V) |
|---|---|---|---|---|---|
| Origin | 1.7888 | 1.8024 | 1.8398 | 0.051 | 0. 4520 |
| $Na^+$ | 1.1270 | 1.1281 | 1.1343 | 0.0073 | -0.0588 |
| $(BO_3)^{3-}$ | 1.6728 | 1.6893 | 1.6939 | 0.0211 | 0.2935 |
| $(BO_4)^{5-}$ | 1.6709 | 1.6890 | 1.6992 | 0.0283 | 0.0922 |
| $(VO_4)^{3-}$ | 1.5334 | 1.5369 | 1.5373 | 0.0039 | 0.3350 |
| Sum | | | | 0.0606 | 0.6619 |

**F. The "new hot spots" as $(VO_4)^{3-}$ groups**

According to anionic group theory, [76] the nonlinear optical effects mainly come from the the most of $(BO_3)^{3-}$ and little of $(BO_4)^{5-}$ anionic groups in the borate crystals. [34, 77] In addition, the distorted $MO_4$ tetrahedron groups such as $(PO_4)^{3-}$, $(SiO_4)^{4-}$, $(ZnO_4)^{4-}$, and $(AlO_4)^{5-}$ are often employed in designing new NLO materials. However, the $(PO_4)^{3-}$, $(SiO_4)^{4-}$, $(ZnO_4)^{4-}$, and $(AlO_4)^{5-}$ anionic groups have little contributions to overall microscopic second-order susceptibilities compared with B-O groups. [78-82]In this paper, using the the SHG-weighted electron density analysis and the real-space atom-cutting technique, the origination of the nonlinear optical properties of NVB has been investigated. As indicated in the above mentioned discussions, the NLO effects of NVB crystal mainly originate from $(VO_4)^{3-}$ rather than $(BO_3)^{3-}$ and $(BO_4)^{5-}$.

It should mentioned that similar result are found in the BIBO[37] and $YAl_3(BO_3)_4$ (YAB) [48] in which the contributions from the $(BiO_4)^{5-}$ and $(YO_6)^{9-}$ groups dominate the microscopic second-order susceptibilities. The SHG density analysis reveals that both Bi and Y cations are not spherical but form significant covalent chemical bonds with the neighbour O anions, establishing the $(BiO_4)^{5-}$ quadrangular pyramids[15] and deformed $(YO_6)^{9-}$ octahedra[48] as "hot spots" contribution to the NLO effect are also much larger than that of $(BO_3)^{3-}$ groups in the BIBO and YAB, respectively.[59] The real-space atom-cutting technique, therefore, clarifies that the NLO effect in these crystals does not mainly originate from the B–O anionic groups, and the contribution from the Bi–O or Y–O groups is even more important. The fact that the contribution of the distorted $(VO_4)^{3-}$ groups is larger than that of $(BO_3)^{3-}$ give a "new hot spots" that besides $(BiO_4)^{5-}$ quadrangular pyramids and deformed $(YO_6)^{9-}$ octahedra, distorted $(VO_4)^{3-}$ groups can also be used to design new NLO compounds with enhanced SHG coefficients.

## Conclusions

On the theoretical front, our comprehensive *ab initio* study of the linear and nonlinear optical properties of NVB agrees very well with the experimental observations. It is shown that the top of the valence bands are dominated by the O 2*p* orbitals, while the bottom of the conduction bands are mainly composed of V 3*d* and B 2*p* orbitals. Based upon the electronic structure, the refractive indices and SHG coefficients were calculated, which are in good agreement with the experimental values. The combined SHG-weighted electron density analysis with the real-space atom-cutting method revealed that the $(BO_3)^{3-}$ anionic groups have a dominant contribution to the linear optical properties, while the $(VO_4)^{3-}$ tetrahedra play a virtual role to the SHG effects in NVB. The theoretical results not only demonstrate that NVB is a potential SHG material for blue wavelength applications, but also identify "new hot spots" $(VO_4)^{3-}$ in addition to the well-known $(BO_3)^{3-}$ that proved to produce large microscopic second-order susceptibilities in this crystal, which is an important hint for future material design.

## Acknowledgements

This work is supported by the National Key Basic Research Program of China (Grant No. 2014CB648400, 2012CB626803), the "Western Light Joint Scholar Foundation" Program of CAS (Grant No. LHXZ201101), the "National Natural Science Foundation of China" (Grant Nos. 11474353, 11104344), the Recruitment Program of Global Experts (1000 Talent Plan, Xinjiang Special Program), Major Program of Xinjiang Uygur Autonomous Region of China during the 12th Five-Year Plan Period (Grant No. 201130111); NCHC for database resources support, and Key Win Electronics Co. for equipment donation and Xinjiang Program of Introducing High-Level Talents are highly appreciated by MHL.

## Notes and references

[a] Key Laboratory of Functional Materials and Devices for Special Environments of CAS; Xinjiang Key Laboratory of Electronic Information Materials and Devices, Xinjiang Technical Institute of Physics & Chemistry of CAS, 40-1 South Beijing Road, Urumqi 830011, China;

[b] University of Chinese Academy of Sciences, Beijing 100049, China;

[c] Department of Physics, Tamkang University, Taipei 25137, Taiwan

† Corresponding Author, email:

zhyang@ms.xjb.ac.cn, slpan@ms.xjb.ac.cn.

Electronic Supplementary Information (ESI) available: [Experimental Details: Crystal Growth, Transmittance Spectrum and Refractive-Index Dispersion Measurements. The distortion of the $VO_4$ tetrahedron in NVB crystal; Crystal transmission spectrum and crystal photograph; The experimental SHG phase matching range; Selected bond lengths (Å) and angles (deg) for the NVB; State energies (eV) of the highest valence band (H-VB) and the lowest conduction band (L-CB) at same *k*-points of NVB; The experimental values of refractive indices were measured several wavelengths at room temperature; The nonzero elements of $\chi(2)$ expected for NVB crystal in point group 222.]. See DOI: 10.1039/b000000x/

1 Chai, B. H. T. Optical Crystals. In CRC Handbook of Laser Science and Technology Supplement 2: Optical Materials; Weber, M. J., Ed.; CRC Press: Boca Raton, FL, 1995; pp 3-65; Chen, C. T., Sasaki, T., Li, R. K., Wu, Y.C., Lin, Z. S., Mori, Y., Hu, Z., Wang, J., Uda, S., Yoshimura, M. and Kaneda, Y., Nonlinear Optical Borate Crystals. Weily-VCH Germany, 2012; pp 1-9.

2 Ok, K. M., Halasyamani, P. S., *Chem. Mater.* 2006, **18**, 3176-3183; Ok, K. M., Chi, E. O. and Halasyamani, P. S., *Chem. Soc. Rev*. 2006, **35**, 710-717.

3 Reshak, Ali H., Auluck, S., Kityk, I. V., Majchrowski, A., Kasprowicz, D., Drozdowski, M., Kisielewski, J., Lukasiewicz, T., Michalski, E. *J Mater Sci.*, 2006, **41**, 1927 –1932.

4 Reshak, Ali H., Auluck, S., Kityk, I. V., *Phys. Rev. B* 2007, **75**, 245120.

5 Reshak, Ali H., Chen, X.A., Auluck, S., Kityk, I. V., *J. Chem. Phys.*2008, **129**, 204111.

6 Reshak, Ali H., Auluck, S., Majchrowski, A., Kityk, I. V., *Solid State Sciences*, 2008, **10**, 1445-1448.

7 Reshak, Ali H., Auluck, S., Kityk, I. V., *Appl. Phys. A*, 2008, **91**, 451–457 .

8 Reshak, Ali H., Chen, X.A., Kityk, I. V., Auluck, S., *Current Opinion in Solid State and Materials Science*, 2007, **11**, 33–39.
9 Reshak, Ali H., Auluck, S., Kityk, I. V., *J. Alloys compounds*, 2008, **460**, 99-102.
10 Reshak, Ali H., Auluck, S., Kityk, I. V., *J. Phys.: Condens. Matter*, 2008, **20,** 145209-145223.
11 Reshak, Ali H., Auluck, S., Kityk, I. V., *Journal of Solid State Chemistry*, 2008,**181**, 789–795.
12 Reshak, Ali H., Chen, X.A., Auluck, S., Kityk, I. V., Iliopoulos, K., Couris, S., Khenatah, R., *Current Opinion in Solid State and Materials Science*, 2009, **12**, 26–31.
13 Reshak, Ali H., Auluck, S., Majchrowski, A., Kityk, I. V., *Jpn. J. Appl. Phys.* 2009, **48**, 011601.
14 Reshak, Ali H., Auluck, S., Kityk, I. V., *J. Phys. D: Appl. Phys.* 2009,**42**, 085406 -085414.
15 Reshak, Ali H., Chen, X. A., Song, F. P., Auluck, S., Kityk, I. V., *J. Phys.: Condens. Matter* 2009, **21**, 205402-205422.
16 Reshak, Ali H., Auluck, S., Kityk, I. V., *J. Phys. Chem. A*, 2009, ***113*** (8), 1614–1622.
17 Reshak, Ali H., Auluck, S., Kityk, I. V., *J. Phys. Chem. B*, 2009, ***113*** (34), 11583–11588.
18 Reshak, Ali H., Atuchin, V V, Auluck, S., Kityk, I. V., *J. Phys.: Condens. Matter* , 2008, **20**, 325234-325266.
19 Reshak, Ali H., Auluck, S., Kityk, I. V., Perona, A., Claudet, B., *J. Phys.: Condens. Matter* , 2008, **20**, 325213-325245.
20 Reshak, Ali H., Auluck, S., *Solid State Communications*, 2008, **145**, 571–576.
21 Reshak, Ali H., Ortíz Andrés Ordóñez, D., *J. Phys. Chem. B* 2009, **113**, 13208–13215.
22 Reshak, Ali H., Khenata, R., Kityk, I. V., Plucinski, K. J., Auluck, S., *J. Phys. Chem. B*, 2009, ***113*** (17), 5803–5808.
23 Reshak, Ali H., Auluck, S., Kityk, I. V., *Current Opinion in Solid State and Materials Science*, 2009, **12**, 14–18.
24 Wu, H. P., Pan, S. L., Poeppelmeier, K. R., Li, H. Y., Jia, D. Z., Chen, Z. H., Fan, X. Y., Yang, Y., Rondinelli, J. M. and Luo, H., *J. Am. Chem. Soc.* 2011, **133**, 7786-7790; Wu, H. P., Yu, H. W., Yang, Z. H., Hou, X. L., Su, X., Pan, S. L., Poeppelmeier, K. R. and Rondinelli, J. M., *J. Am. Chem. Soc.*, 2013, **135**, 4215-4218; Wu, H. P., Yu, H. W., Pan, S. L., Huang, Z. J., Yang, Z. H., Su, X. and Poeppelmeier，K. R., *Angew. Chem. Int. Ed.*, 2013, **52**, 3406-3410; Li, F, Pan, S. L., Hou, X. L. and Zhou, Z. X. *J. Crystal Growth* 2010, **312**, 2383; Li, F, Pan, S. L., *J. Crystal Growth* 2011, **318**, 629.
25 Ra, H. S., Ok, K. M. and Halasyamani, P. S., *J. Am. Chem. Soc.* 2003, **125**, 7764-7765; Sun, C. F., Hu, C. L., Xu, X., Yang, B.-P. and Mao, J. G., *J. Am. Chem. Soc.* 2011, **133**: 5561-5572; Zhang, J., Zhang, Z., Zhang, W., Zheng, Q., Sun, Y., Zhang, C. Q. and Tao, X. T., *Chem. Mater.* 2011, **33**, 3752-3761; Huang, Y. Z., Wu, L. M., Wu, X. T., Li, L. H., Chen, L. and Zhang, Y. F., *J. Am. Chem. Soc.* 2010, **132**, 12788-12789; Zhang, W.L., Cheng, W. D., Zhang, H., Geng, L., Lin, C. S. and He, Z. Z., *J. Am. Chem. Soc*. 2010, **132**, 1508-1509;
26 Kunz, M. and Brown, I. D., *J. Solid State Chem.* 1995, **115**, 395-406.
27 Goodenough, J. B. and Longo, J. M.: *Crystallographic and magnetic properties of perovskite and perovskite-related compounds*. In Landolt-Bornstein; Hellwege, K. H., Hellwege, A. M., Eds.; Springer-Verlag: Berlin, 1970; Vol. **4**, pp 126-314.
28 Touboul, M., Penin, N. and Nowogrocki, G., *J Solid State Chem.* 2000, **150**, 342-346.
29 Chen, S. J., Pan, S. L., Zhao, W. W. and Yu, H. W., *Dalton Trans.*. 2012, **41**, 9202-9208.
30 Fan, X. Y., Pan, S. L., Han, J., Tian, X. L. and Zhou, Z. X., *J. Syn. Cryst.* 2010, **39**, 35-42.
31 Fan, X. Y., Pan, S. L., Hou, X. L., Tian, X. L. and Han, J., *Cryst. Growth* 2010, **312**, 2263-2266.
32 Fan, X. Y., Pan, S. L., Hou, X. L., Tian, X. L. and Han, J., *Cryst. Growth Des*. 2010, **10**, 252- 256.
33 Chen, C. T., Wu, B. C., Jiang, A. and You, G., *Sci. Sin. B*. 1985, **28**, 235.
34 Lin, Z. S., Lin, J., Wang, Z. Z., Chen, C. T. and Lee, M. H., *Phys. Rev. B* 2000, **62**, 1757.
35 Lin, Z. S., Wang, Z. Z., Chen, C. T., Chen, S. K. and Lee, M. H., *Chem. Phys. Lett*. 2003, **367**, 523-527.
36 Lin, Z. S., Wang, Z. Z., Chen, C. T., Chen, S. K. and Lee, M. H., *J. Appl. Phys*. 2003, **93**, 9717-9723.
37 Lin, Z. S., Wang, Z. Z., Chen, C. T. and Lee, M. H., *J. Appl. Phys*. 2001, **90**, 5585.
38 Lin, Z. S., Wang, Z. Z., Chen, C. T. and Lee, M. H., *Acta Phys. Sin*. 2003, **50**, 1145-1149.
39 Lin, Z. S., Wang, Z. Z., Chen, C. T. and Lee, M. H., *Chem. Phys*. 2003, **118**, 2349-2356.
40 Clark, S. J., Segall, M. D., Pickard, C. J., Hasnip, P. J., Probert, M. J., Refson, K. and Payne, M. C., *Z. Kristallogr.* 2005, **220**, 567-570.
41 Pfrommer, B. G., Cote, M., Louie, S. G. and Cohen, M. L., *J. Comput. Phys.*1997, **131**, 233-240.
42 Perdew, J. P., Burke, K. and Ernzerhof, M., *Phys. Rev. Lett.* 1996, **77**, 3865-3868.
43 Lin, J. S., Qteish, A., Payne, M. C. and Heine, V., *Phys. Rev. B.* 1993, **47**, 4174-4180.
44 Rappe, A. M., Rabe, K. M., Kaxiras, E. and Joannopoulos, J. D., *Phys. Rev. B* 1990, **41**, 1227-1230.
45 Monkhorst, H. J. and Pack, J. D., *Phys. Rev. B* 1976, **13**, 5188-5192.
46 Cococcioni, M and de Gironcoli, S., *Phys. Rev. B* 2005, **71**, 035105-035121.
47 Dudarev, S. L., Botton, G. A., Savrasov, S. Y., Humphreys, C. J. and Sutton, A. P., *Phys. Rev. B* 1998, **57**, 1505-1509.
48 He, R., Lin, Z. S., Lee, M. H. and Chen, C. T., *J. Appl. Phys*. 2011, **109**, 103510-103515
49 Palik, E. D., *Handbook of Optical Constants of Solids*. Orlando: Academic Press: New York, 1985.
50 Wooten, F. *Optical Properties of Solid* (Academic, New York, 1972)
51 Lee, M. H., Yang, C. H. and Jan, J. H., *Phys. Rev. B* 2004, **70**, 235110-235121.
52 Huang, H., Lin, Z. S., Bai, L., Hu, Z. G. and Chen, C. T., *J. Appl. Phys.* 2009, **106**, 103107-103112.
53 Kunz, Martin and Brown David I., *J. Solid State Chem.* 1995, **115**, 395-406.
54 Su, X., Wang, Y., Yang, Z. H., Huang, X. C., Pan, S. L., Li, F. and Lee, M. H., *J. Phys. Chem. C* 2013, **117**, 14149-14157.
55 Zhang, B.B.,Yang, Z. H., Yang, Y., Lee, M. H., Pan, S. L., Jing, Q. and Su, X., *J. Mater. Chem. C* 2014, **2**, 4133-4141.
56 Jing, Q., Dong, X. Y., Yang, Z. H., Pan, S. L., Zhang, B. B., Huang, X.C. and Chen, M. W., *J. Solid State Chem.*, 2014, **219**, 138–142.
57 Lin, Z. S., Lin, J., Wang, Z. Z., Wu, Y. C., Ye, N., Chen, C. T., Li, R. K. *J. Phys.: Condens. Matter* 2001, **13** 369–384.
58 Wang, D.S. *Bull. Mater. Sci.*2003, **26**, 159-163.
59 Lin, Z. S., Jiang, X. X., Kang, L., Gong, P. F., Luo, S.Y. and Lee, M. H., *J. Phys. D: Appl. Phys.* 2014, **47**, 253001-253019.
60 Halasyamani, P. S., *Chem. Mater.* 2004, **16**, 3586-3592. And references cited therein.



 

61 Touboul, M., Denis, S. and Seguin, L., *Eur. J. Solid State Inorg. Chem.* 1995, **32**, 577-588.
62 Touboul, M., Melghit, K., Bénard, P. and Loüer, D., *J. Solid State Chem.* 1995, **118**, 93-98.
63 Touboul, M. and Tolédano, P., *Acta Crystallogr. Sect. B: Struct. Sci.* 1980, **36**, 240-255.
64 Touboul, M. and Tolédano, P., *J. Solid State Chem*. 1981, **38**, 386-393.
65 Yahia, Hamdi Ben, Gaudin, Etienne and Darriet, Jacques., *Inorg. Chem.* 2005, **44**, 3087-3093.
66 Rashkeev, S. N., Lambrecht, W. R. L. and Segall, B., *Phys. Rev. B* 1998, **57**, 3905-3919.
67 Rashkeev, S. N. and Lambrecht, W. R. L., *Phys. Rev. B* 2001, **63**, 165212-165224.
68 Chen, C.W., Lee, M. H. and Lin, Y. T., *Appl. Phys. Lett*. 2006, **89**, 223105-223108.
69 Dmitriev, V. G., Gurzadyan, G. G. and Nikogosyan, D. N. *Handbook of Nonlinear Optical Optical Crystals*; Springer-Verlag Berlin Heidelberg 2008; pp 22-29; (b) Aversa, C. and Sipe, J. E., *Phys. Rev. B* 1995, **52**, 14636-14645.
70 Chen, C. T., Wu, Y. C., Jiang, A. D., You, G. M., Li, R. K. and Lin, S. J., *J. Opt. Soc. Am. B* 1989, **6**, 616-621.
71 Wu, B. C., Tang, D. Y., Ye, N. and Chen, C. T., *Opt. Mater.* 1996, **5**, 105-109.
72 Goodey, J., Broussard, J. and Halasyamani, P. S., *Chem. Mater*. 2002, **14**, 3174.
73 Rashkeev, S. N. and Lambrecht, W. R., *Phys. Rev. B* 2001, **63**, 165212.
74 Lin, J., Lee, M. H., Liu, Z.P., Chen, C.T. and Pickard, C. J., *Phys. Rev. B* 1999, **60**, 13380-13389.
75 Lo, C. H. and Lee, M. H.: *The Role of Electron Lone-pair in the Optical Nonlinearity of Oxide, Nitride and Halide Crystals* (Master Thesis, Taiwan 2005), p29.
76 Chen, C. T., Ye, N., Lin, J., Jiang, J., Zeng, W. R. and Wu, B. C., *Adv. Mater.*1999, **11**, 1071-1078.
77 Chen, C. T. *Development of New Nonlinear Optical Crystals in the Borate Series*, edited by Letokhov, V. S.; Shank, C. V.; Shen, Y. R. and Walther H. (Harwood Academic, Chur, 1993).
78 Zhang, E. P., Zhao, S. G., Zhang, J. X. Fu, J. P. and Yao, J. Y. *Acta Cryst.* 2011, **67,** i3.
79 Lei, B. H., Jing, Q., Yang, Z. H., Zhang, B. B., Pan, S. L., *J. Mater. Chem. C* 2014DOI: 10.1039/C4TC02443E.
80 Wu, H. P.; Yu, H. W.; Pan, S. L.; Huang, Z. J.; Yang, Z. H.; Su, X.; Poeppelmeier, K. R. *Angew. Chem. Int. Ed.* 2013, **52**, 3406 –3410.
81 Lin, Z. S., Wang, Z. Z., Chen, C. T., Chen, S. K.Y. and Lee, M. H. *J. Appl. Phys.* 2003, **93**, 9717–9723.
82 Huang, H, Lin, Z. S., Bai L, Hu, Z. G. and Chen, C. T. *J. Appl. Phys*. 2009,**106**,103107.